

A Novel Transmission Scanner Framework for Real-Time Applications

Dirk Kolb^{1,2}, Ulla Uebler¹, Elmar Nöth²

1 - MEDAV GmbH, Gräfenberger Str. 32-34, 91080 Uttenreuth, Germany

2 - Pattern Recognition Lab, Department of Computer Science, Friedrich-Alexander-University
Erlangen-Nuremberg, Martensstr. 3, 91058 Erlangen, Germany

dirk.kolb@medav.de, ulla.uebler@medav.de, noeth@informatik.uni-erlangen.de

ABSTRACT

The strong need for a robust and real-time transmission classification can be found both in civil and non-civil applications. In this paper, we propose a new technique based on modern and low-complexity object detection approaches. The transmission scanner uses a combination of Haar-like and technical features to detect and classify different, co-occurring narrowband transmissions within wideband signals. The transmission scanner is evaluated with recorded real world data in order to fulfill real conditions. The evaluation shows that this system performs very well with 99.5% accuracy.

1.0 INTRODUCTION

To know what is on air has always been a strong interest of civil and non-civil institutions. The civil area of research has the aim to detect white spaces in frequency bands in order to establish secondary usage, as it is done in Cognitive Radio (CR) [1, 2]. In contrast to this, the non-civil institutions try to identify every signal or a special type of signal. This signal interception is called Communications Intelligence (COMINT). Both benefit from increasing instantaneous receiver bandwidths, made possible by Software-Defined Radio (SDR) [3]. The wider the bandwidth, the higher the knowledge gain can be. The drawback of such a wideband receiver is that the requirements for a real-time signal processing in CR and COMINT applications are higher than before, as the search space increases.

In Fig. 1 the traditional procedural method is shown. A Wideband Receiver (WBR) digitizes the antenna signal with a specific sampling frequency. The typical sampling frequencies for the High Frequency (HF), Very and Ultra High Frequency (VUHF) bands vary between $f_S = 625$ kHz and $f_S = 20$ MHz. The discretized signal is led to a Wideband Signal Detection (WDET). The most approaches for this stage are based on an energy detection. They use no a knowledge to extract the information regarding the center frequency, bandwidth, transmission start and duration. The information of WDET is used within the Digital Down Conversion (DDC) to cut the narrowband signals out of the wideband signal and transfer them to the Narrowband Transmission Classification (NTCL). The NTCL extracts specific features, e. g., modulation type and baud rate, in order the get the information about the used transmission standard, e. g., STANAG-4285 or PACTOR II [4]. Approaches for the modulation classifier are presented in [5–8]. The evaluation of most of these algorithms has been done without consideration of inaccuracies of the first stage and furthermore almost all test signals have been created without consideration of transmission standards. Therefore, two problems

Report Documentation Page			Form Approved OMB No. 0704-0188		
Public reporting burden for the collection of information is estimated to average 1 hour per response, including the time for reviewing instructions, searching existing data sources, gathering and maintaining the data needed, and completing and reviewing the collection of information. Send comments regarding this burden estimate or any other aspect of this collection of information, including suggestions for reducing this burden, to Washington Headquarters Services, Directorate for Information Operations and Reports, 1215 Jefferson Davis Highway, Suite 1204, Arlington VA 22202-4302. Respondents should be aware that notwithstanding any other provision of law, no person shall be subject to a penalty for failing to comply with a collection of information if it does not display a currently valid OMB control number.					
1. REPORT DATE SEP 2010		2. REPORT TYPE N/A		3. DATES COVERED -	
4. TITLE AND SUBTITLE A Novel Transmission Scanner Framework for Real-Time Applications				5a. CONTRACT NUMBER	
				5b. GRANT NUMBER	
				5c. PROGRAM ELEMENT NUMBER	
6. AUTHOR(S)				5d. PROJECT NUMBER	
				5e. TASK NUMBER	
				5f. WORK UNIT NUMBER	
7. PERFORMING ORGANIZATION NAME(S) AND ADDRESS(ES) MEDAV GmbH, Gräfenberger Str. 32-34, 91080 Uttenreuth, Germany				8. PERFORMING ORGANIZATION REPORT NUMBER	
9. SPONSORING/MONITORING AGENCY NAME(S) AND ADDRESS(ES)				10. SPONSOR/MONITOR'S ACRONYM(S)	
				11. SPONSOR/MONITOR'S REPORT NUMBER(S)	
12. DISTRIBUTION/AVAILABILITY STATEMENT Approved for public release, distribution unlimited					
13. SUPPLEMENTARY NOTES See also ADA568727. Military Communications and Networks (Communications et reseaux militaires). RTO-MP-IST-092					
14. ABSTRACT The strong need for a robust and real-time transmission classification can be found both in civil and non-civil applications. In this paper, we propose a new technique based on modern and low-complexity object detection approaches. The transmission scanner uses a combination of Haar-like and technical features to detect and classify different, co-occurring narrowband transmissions within wideband signals. The transmission scanner is evaluated with recorded real world data in order to fulfill real conditions. The evaluation shows that this system performs very well with 99.5% accuracy.					
15. SUBJECT TERMS					
16. SECURITY CLASSIFICATION OF:			17. LIMITATION OF ABSTRACT SAR	18. NUMBER OF PAGES 14	19a. NAME OF RESPONSIBLE PERSON
a. REPORT unclassified	b. ABSTRACT unclassified	c. THIS PAGE unclassified			

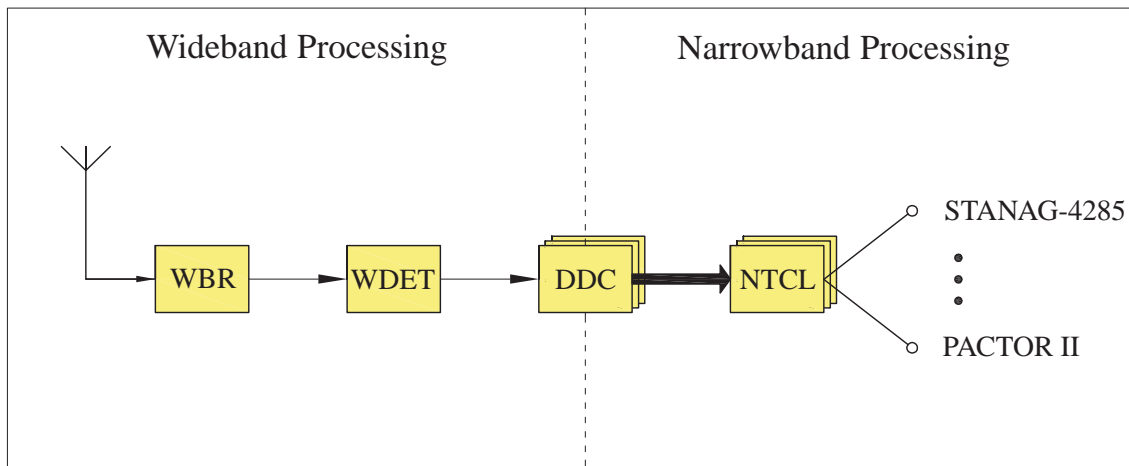


Figure 1: Processing chain with separated wideband signal detection and narrowband transmission classification.

arise in real applications. First, most of the classification approaches used in NTCL extract features or technical parameters which lose their quality in case of detection inaccuracies, e. g., frequency offset. Second, several transmission standards, e. g., STANAG-4285 [4], change the modulation index or the type during the transmission, or use a double modulation, e. g., PACKET-RADIO [4]. Therefore, a feature, which is able to distinguish specific modulation types, might fail in applications where a signal with different modulation types commonly occurs. The biggest problem of the block diagram shown in Fig. 1 is the separation of wideband and narrowband processing. The resulting quality of signal detectors degrades in case of lower signal-to-noise ratios (SNRs) or stronger fading effects. This leads to incorrect information for the DDC block and to useless narrowband signals for the NTCL stage. In most of the cases the classification results are incorrect. Thus, it is advisable to avoid a separation between wideband and narrowband processing or to combine signal detection and classification.

With tremendously increased processing power, more research has been done in SDR in the last years. Especially in the area of SDR and CR new strategies of an improved combined detection and classification emerged. Beside the typical energy based detectors [9] the first detectors using a priori knowledge came up. These detectors are based on features, for example, second-order cyclostationarity [10, 11] or higher-order statistics. They are reliable even at lower SNRs, but the computational effort is very high. Within the presented literature it is mostly assumed that the center frequencies of the signals of interest are well known, which is true for most so-called cooperative applications. In non-civil or non-cooperative applications the only assumption that can be made is that there might be a signal of interest at an unknown position. This requires a scanning classification system which is possible to perform the scanning and classification process in real-time.

In this paper we present a flexible combined transmission detection and classification for both cooperative and non-cooperative applications. It will be trained for a common HF transmission standard. The system is evaluated with real signals in order to show the robustness.

The paper is organized as follows: Section 2.0 describes the principle of transmission scanning. In Section 2.1, we present the features used for the classification. Section 2.2 analyzes the classification system.

Section 3.0 reports on the performance of our system. In Section 4.0, we present conclusions along with recommendations for future improvements.

2.0 TRANSMISSION SCANNER FRAMEWORK

The basis of our approach is the spectrogram of a wideband signal. In Fig. 2 only a small part of a wideband spectrogram is shown. Many experts are able to detect and classify transmissions only by looking at this special visualization. Thus, the principle of our proposed transmission scanner is comparable to well-known object detection techniques (e. g., face detection [12]), which are applied to images. In short, the scan is a series of detections and classifications of different masks which are moved over the image. In our case, the image is comparable with the complex spectrogram \mathbf{X}

$$\mathbf{X} = \begin{bmatrix} \mathbf{x}_1 \\ \vdots \\ \mathbf{x}_i \\ \vdots \\ \mathbf{x}_{t_N} \end{bmatrix} = \begin{bmatrix} X[1,1] & \dots & X[1,j] & \dots & X[1,f_{\text{FFT}}] \\ \vdots & \ddots & \vdots & & \\ X[i,1] & \dots & X[i,j] & \dots & X[i,f_{\text{FFT}}] \\ \vdots & & \vdots & \ddots & \\ X[t_N,1] & \dots & X[t_N,j] & \dots & X[t_N,f_{\text{FFT}}] \end{bmatrix}, \quad (1)$$

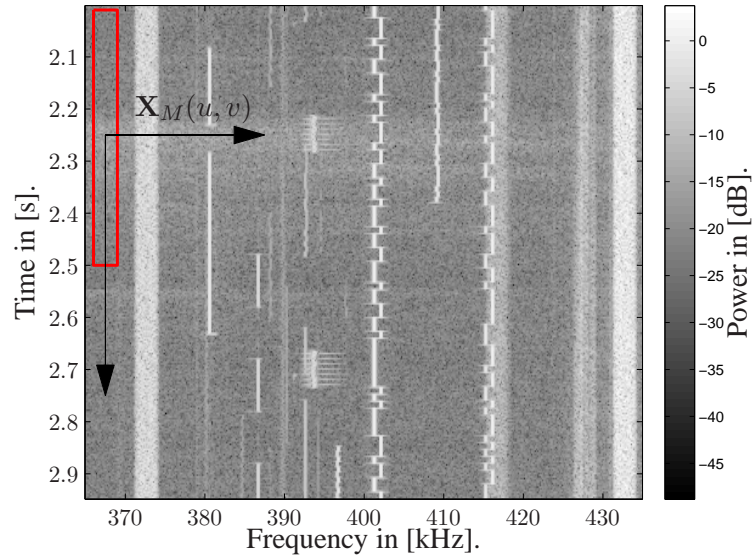
where $|\mathbf{x}_i|$ are the bins of the power spectrum and t_N is the number of short-time spectrums used for classification. \mathbf{x}_i is computed within the wideband receiver, a ComCatTM-Tuner delivered by MEDAV [13]. With an applied FFT length $f_{\text{FFT}} = 4096$ samples, a sampling frequency $f_S = 625$ kHz and a Hann window with 50% overlapping, we receive a frequency resolution $\Delta f = 153$ Hz and a time resolution $\Delta t = 0.003$ sec¹. The mentioned mask is fitted to the transmission we are looking for. In Section 3.0 the transmission of interest is a STANAG-4285 signal. It is a continuous, fixed frequency and 3.0 kHz wide signal. It became evident that 0.500 s signal length is sufficient for a robust classification. Thus, the mask is 3.3 kHz wide and 0.500 sec long. Lower time lengths are possible, but will result in a lower classification rate. This leads to a mask \mathbf{X}_M , $f_M = 22$ bins wide and $t_M = 168$ bins long,

$$\mathbf{X}_M(u, v) = \begin{bmatrix} X[u, v] & \dots & X[u, v + f_M] \\ \vdots & \ddots & \vdots \\ X[u + t_M, v] & \dots & X[u + t_M, v + f_M] \end{bmatrix}, \quad (2)$$

where $u = [1, \dots, t_N - t_M]$ is the position in time direction and $v = [1, \dots, f_{\text{FFT}} - f_M]$ the position in frequency direction of \mathbf{X} . In Fig. 3 the block diagram for the new system is shown. By sweeping of \mathbf{X}_M or rather varying u and v , all possible mask positions within \mathbf{X} are sent to the wideband feature extraction and then to the wideband classification. The wideband feature extraction is described in Section 2.1 and the wideband classification in Section 2.2.

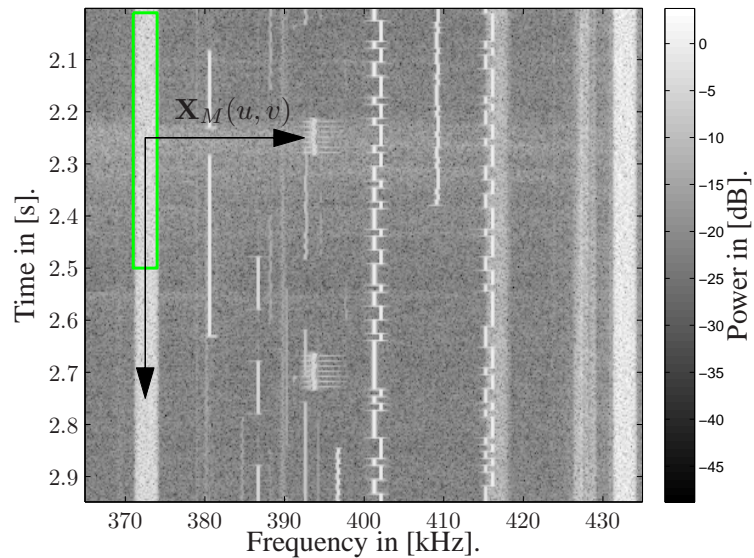
¹These resolutions are adapted to the High Frequency (HF) range. For the Very and Ultra High Frequency (VUHF) bands other resolutions should be chosen.

Spectrogram of multiple transmissions.



(a)

Spectrogram of multiple transmissions.



(b)

Figure 2: Part of an absolute, logarithmic wideband spectrogram. It contains several transmissions, for example, STANAG-4285 and BAUDOT. A STANAG-4285 mask X_M with $f_M = 22$ bins and $t_M = 168$ bins is exemplarily swept over the spectrogram. In Fig. 2(a) X_M lies not on a STANAG-4285 transmission. In Fig. 2(b) X_M lies on a STANAG-4285 transmission.

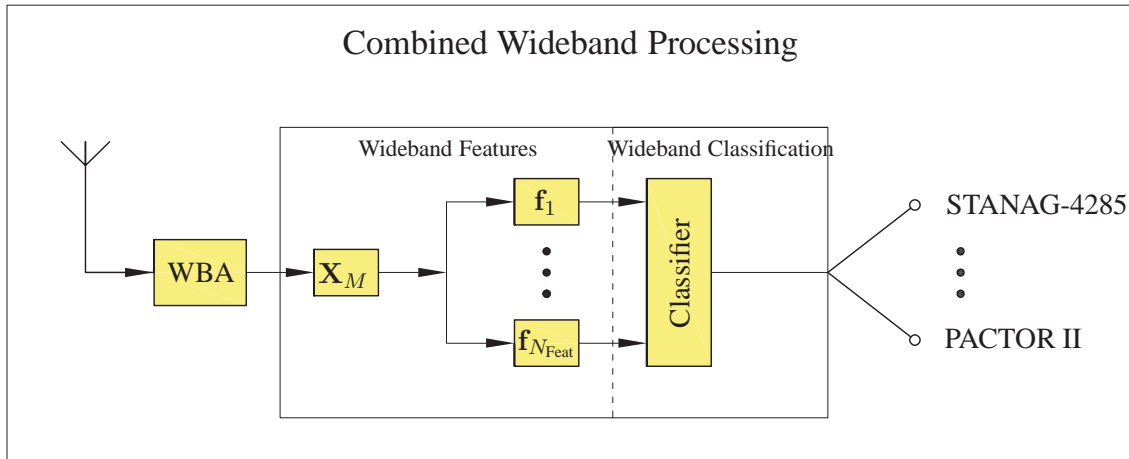


Figure 3: Processing chain with a combined wideband signal detection and transmission classification.

2.1 Wideband Features

For transmission classification, it is desirable to define N_{Feat} different feature types. There are features which are very efficient but not definite, and there are features which allow exact decisions but are very inefficient. Thus, the proposed framework gives us the possibility to include different feature groups and to benefit from the different advantages. At the end of the feature extraction, we obtain a feature vector \mathbf{f}

$$\mathbf{f} = [\mathbf{f}_1, \dots, \mathbf{f}_{N_{\text{Feat}}}] \quad (3)$$

with N

$$N = N_1 + \dots + N_{N_{\text{Feat}}} \quad (4)$$

dimensions.

In the research area of object detection optical features, like Haar-like features, are state of the art. They are very efficient and obtain a good quality. In our approach, we apply the Haar-like features to the logarithmic, absolute mask $\mathbf{X}_{M,\log}$

$$\mathbf{X}_{M,\log} = 10 \cdot \log_{10} \left(|\mathbf{X}_M|^2 \right). \quad (5)$$

The original, complex mask \mathbf{X}_M gives us the possibility to extract more information, which is invisible in the logarithmic, absolute spectrogram. In addition to the optical Haar-like features, we use technical, phase-related features, too.

2.1.1 Haar-like Features

The evaluation of every single bin within the mask does not give any information other than signal power and phase information, which is not sufficient for the classification process. So, first of all we need features that encode the relation of different signal power values within one observed mask $\mathbf{X}_{M,\log}$. Haar-like features are typically used to describe contrasts within images. Applied to our problem, these features characterize the two-dimensional energy distribution.

Our Haar-like feature, which is shown in Fig. 4, set was inspired by Papageorgiou *et al.* in [14]. We reduced the number of Haar-like features to a radio signal specific set. It contains now 20 2-D windows, and can be used for different transmission types. Depending on the Haar-feature that is used for extraction, different tasks can be fulfilled. Fig. 4(f) and Fig. 4(g) are for the symbol alternations of a 2-FSK transmission, whereas Fig. 4(h) is useful for the bandwidth estimation.

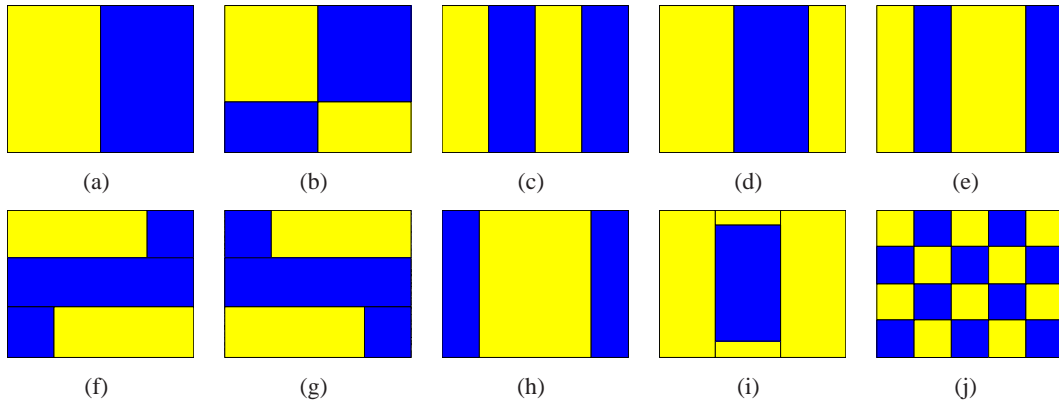


Figure 4: Haar-like features used for detection and classification. Dark-colored areas have negative and light-colored areas positive weights.

The Haar-like features are applied to different positions with variable scale factors within the mask \mathbf{X}_M , as it shown in Fig. 5. In this case, the resulting feature value is the difference between the rectangle A and rectangle B . Considering all possible positions and scaling factors, $N_{\text{Haar}} = 362.720$ Haar-like features are extracted. Viola *et al.* showed in [12] a very fast computation scheme based on integral images, which has been adapted in our implementation.

2.1.2 Phase-related Feature

In this paper we introduce a technical feature which is especially suited to detect periodic sequences within a transmission. These sequences are part of the standard and often used, in order to enable equalization algorithms. This feature is based on a cepstral analysis, which is suitable for the detection of periodic values, as described by Bogert *et al.* in [15]. In contrast to the cyclostationary feature, presented by Gardner *et al.* in [10], the cepstral feature is modulation type independent. Thus, it is suitable for transmissions with changing modulation types or double modulated content. Additionally, the distance between training sequences is often unique for different transmission standards. The cepstrum $q_{\text{Ceps}}(t)$ of a complex signal

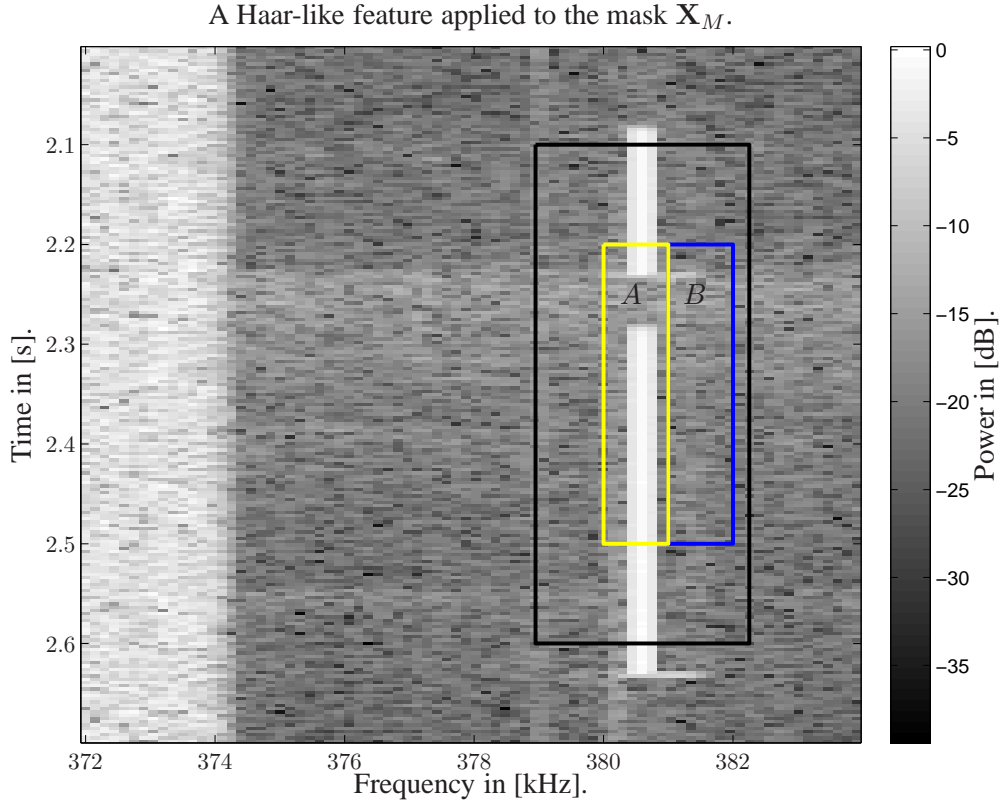


Figure 5: The Haar-like feature, which is shown in Fig. 4(a), is applied to the mask \mathbf{X}_M at a certain position and with specific scaling factors.

$q(t)$ can be expressed as a function, as follows

$$q_{\text{Ceps}}(t) = \left| \int_{-\infty}^{+\infty} \log \left(|Q(w)|^2 \right) e^{-j\omega t} d\omega \right|^2, \quad (6)$$

where $Q(w)$ is

$$Q(w) = \int_{-\infty}^{+\infty} q(t) e^{-j\omega t} dt. \quad (7)$$

In our case, $q(t)$ is the downsampled narrowband signal, dependent on the position of the mask \mathbf{X}_M within \mathbf{X} . In Fig. 6 the cepstrum of two transmissions is plotted. It shows the position of a training sequence and its harmonics. Exploiting the harmonic structure within the cepstrum, the distance between the sequences can be extracted and used for classification. In both cases a peak analysis gives the correct result of 106.6 msec between the sequences. In Fig. 6(b) it emerged that the cepstrum is very robust against fading and low SNR. With $N_{\text{Cepst}} = 1$, we obtain a feature vector \mathbf{f} with $N = 362.721$ different elements.

2.2 Wideband Classifier

Given a set of labeled feature vectors, which are computed from the signal and rejection patterns, any machine learning approach can be used to learn a functional relationship between feature values and classes.

Although the Haar-like features can be computed very efficiently, extracting the complete set is very expensive. So, we decided to use the *Adaptive Boosting* (AdaBoost) algorithm, which is well-known in object detection and first published by Freund *et al.* in [16]. AdaBoost trains T weak classifiers $h_t(\mathbf{X}_M)$ repeatedly with $t = 1, \dots, T$. The final strong classifier is a weighted combination of the iterated hypotheses h_t . Generally, for every iteration a weak classifier which evaluates a threshold Θ_t on a single feature f_t is trained to distinguish between the signal class c_1 and the rejection class c_2 :

$$h_t(\mathbf{X}_M) = \begin{cases} c_1, & f_t(\mathbf{X}_M) < \Theta_t \\ c_2, & \text{otherwise} \end{cases} \quad (8)$$

After each iteration, the training set is reweighted with respect to the error rate of the last weak classifier. As T is chosen to be smaller than the overall number of available features N , the number of features will be reduced during the training process. N' will remain after the training:

$$N' \ll N \text{ with } N' = N'_{\text{Haar}} + N'_{\text{Cepst}}. \quad (9)$$

It can happen that N'_{Haar} or N'_{Cepst} is zero. In this case the corresponding feature group will not be used for the classification process. For more details regarding AdaBoost, see [16].

3.0 EXPERIMENTAL RESULTS

The task is to detect STANAG-4285 transmissions in wideband signals without prior knowledge, e. g., the exact position, and reject noise and all other transmissions. For the experiments, we trained three different, monolithic AdaBoost classifiers with $T = 10$ weak classifiers. The first classifier is trained with both feature groups \mathbf{f}_{Haar} and \mathbf{f}_{Ceps} , while the others are trained each with feature group \mathbf{f}_{Haar} or \mathbf{f}_{Ceps} .

Unfortunately, there exists no realistic labeled data from real-world transmissions. Thus, the wideband signals used for this work were acquired and manually labeled by MEDAV. Researchers, interested in a comparison with their own approach, can have access to the data upon request. The wideband signal for training has a sampling frequency $f_s = 625$ kHz and a center frequency $f_c = 8.350$ MHz. The wideband signal for the evaluation has the same sampling frequency but a center frequency of $f_c = 8.800$ MHz. To provide typical rejection samples for this scenario, the rejection class contains examples of noise and examples of common HF transmissions, e. g., SITOR-ARQ, BAUDOT, GW-PACTOR, GW-OFDM, J3E-USB and A1E (described by Prösch in [4]). The used wideband signals are an important part of the realistic evaluation, as they represent a typical HF scenario. They contain a lot of unknown transmissions and time-variant wideband noise. In Table 1 the class distribution is shown.

Table 2 shows the results of the evaluation. Compared to the trainings with only one feature group, we obtained the best classification rate of 99.5% for real world scenarios with the combination of \mathbf{f}_{Haar} and \mathbf{f}_{Ceps} . In Fig. 7, only a part of the results is plotted.

The total positive rate for the rejection class is about 99.7%, and the total positive rate for the signal class is 96.3%. This indicates the fact that the combination of both groups is necessary for a robust classification. A high accuracy for the rejection class is highly appreciated in COMINT applications, because the post processing of missclassified signals is very expensive.

Class	Name	Training	Test
c_1	STANAG-4285	4887	1581
c_2	NOISE	12434	4646
c_2	SITOR-ARQ	2898	2844
c_2	GW-PACTOR	13386	6960
c_2	BAUDOT	5544	6336
c_2	GW-OFDM	9504	5244
c_2	J3E-USB	2088	7032
c_2	A1E	8730	0

Table 1: Number of patterns for training and test set. Due to the realistic properties of the wideband signals, it is possible that some classes have more or less samples, e.g., A1E. Both training and test set contain transmissions with a SNR between 7 dB and 30 dB.

Training and evaluation for $T = 10$						
Feature vector $[f_{\text{Haar}}, f_{\text{Ceps}}]$	TP Rate	FP Rate	Precision	Recall	F-Measure	
$c_1 = \text{STANAG-4285}$	0.963	0.003	0.932	0.963	0.947	
$c_2 = \text{REJECTION}$	0.997	0.037	0.998	0.997	0.997	
Weighted Avg.	0.995	0.035	0.995	0.995	0.995	
Feature vector $[f_{\text{Haar}}]$	TP Rate	FP Rate	Precision	Recall	F-Measure	
$c_1 = \text{STANAG-4285}$	0.822	0.019	0.671	0.822	0.738	
$c_2 = \text{REJECTION}$	0.981	0.178	0.991	0.981	0.986	
Weighted Avg.	0.973	0.171	0.977	0.973	0.975	
Feature vector $[f_{\text{Ceps}}]$	TP Rate	FP Rate	Precision	Recall	F-Measure	
$c_1 = \text{STANAG-4285}$	0.917	0.015	0.745	0.917	0.822	
$c_2 = \text{REJECTION}$	0.985	0.083	0.996	0.985	0.990	
Weighted Avg.	0.982	0.080	0.985	0.982	0.983	

Table 2: Evaluation of the classifiers with real world signals. All possible combinations of the feature groups f_{Haar} and f_{Ceps} have been considered.

Using the integral feature computation and some other optimizations, we could greatly reduce the complexity. We have been able to run about 13.108 classifications per second², which is a great step to real-time CR and COMINT applications.

4.0 SUMMARY AND OUTLOOK

The paper introduced a novel method for transmission scanning based on well-established object detection techniques. In order to improve the accuracy we used beside the typical Haar-like features, also a new cepstral feature. A combination of both feature groups exploited the particular benefits. An adaptation to new transmissions or to VUHF scenarios is possible at any time. With signal recordings provided by MEDAV, we could show that the system performs successfully and very fast under real circumstances. We obtained very good results for a common, real HF scenario.

²A single threaded implementation ran on a Intel®Core™2 Duo CPU T8300 at 2.40 GHz.

In future we will implement an efficient multiclass version of the transmission scanner, based on feature sharing. In order to show the flexibility of our system, we will focus on VUHF transmission standards.

REFERENCES

- [1] Mitola III, J. and Maguire, Jr., G., "Cognitive Radio: Making Software Radios More Personal," *Personal Communications, IEEE*, Vol. 6, No. 4, Aug 1999, pp. 13–18.
- [2] Mitola III, J., "Cognitive Radio for Flexible Mobile Multimedia Communications." *MONET*, Vol. 6, No. 5, 2001, pp. 435–441.
- [3] Mitola III, J., "'Software Radios: Survey, Critical Evaluation and Future Directions,'" *Aerospace and Electronic Systems Magazine, IEEE*, Vol. 8, No. 4, Apr 1993, pp. 25–36.
- [4] Prösch, R., *Technical Handbook For Radio Monitoring I*, Book on Demand GmbH, 1st ed., 2007.
- [5] Azzouz, E. and Nandi, A., *Automatic Modulation Recognition of Communication Signals*, Kluwer Academic Publishers, 1996.
- [6] Fargues, M. and Hatzichristos, G., "A Hierarchical Approach to the Classification of Digital Modulations in Multipath Environments," Tech. rep., Department of Electrical and Computer Engineering, May 2001, NPS-EC-01-004.
- [7] Wikström, M., "A Survey of Modulation Classification Methods for QAM Signals," Tech. rep., Command and Control Systems, 2005.
- [8] Dobre, O., Abdi, A., Bar-Ness, Y., and Su, W., "A Survey of Automatic Modulation Classification Techniques: Classical Approaches and New Trends," *IET Communications*, Vol. 1, 2007, pp. 137–156.
- [9] Digham, F., Alouini, M., and Simon, M., "On the Energy Detection of Unknown Signals Over Fading Channels," *IEEE Transactions on Communications*, Vol. 55, No. 1, 2007.
- [10] Gardner, W. and Spooner, C., "Cyclic spectral analysis for signal detection and modulation recognition," *Military Communications Conference, 1988. MILCOM 88, Conference record. '21st Century Military Communications - What's Possible?'. 1988 IEEE*, Vol. 2, Oct 1988, pp. 419–424.
- [11] Gardner, W., "Exploitation of spectral redundancy in cyclostationary signals," *Signal Processing Magazine, IEEE*, Vol. 8, No. 2, Apr 1991, pp. 14–36.
- [12] Viola, P. and Jones, M., "Robust Real-Time Face Detection." *Int. J. Comput. Vision*, Vol. 57, No. 2, 2004, pp. 137–154.
- [13] MEDAV GmbH, "ComCatTM-Tuner - CCT-NG," 2006.
- [14] Papageorgiou, C., Oren, M., and Poggio, T., "A General Framework for Object Detection," *ICCV*, 1998, pp. 555–562.
- [15] Bogert, B., Healy, M., and Tukey, J., "The Frequency Analysis of Time Series for Echoes: cepstrum, pseudo-Autocovariance, Cross-Cepstrum, and saphe cracking," *Proc. Symp. Time Series Analysis, Ed.: M. Rosenblatt, John Wiley*, 1963, pp. 209–243.

- [16] Freund and Schapire, "A Decision-Theoretic Generalization of On-Line Learning and an Application to Boosting." *JCSS: Journal of Computer and System Sciences*, Vol. 55, 1997.

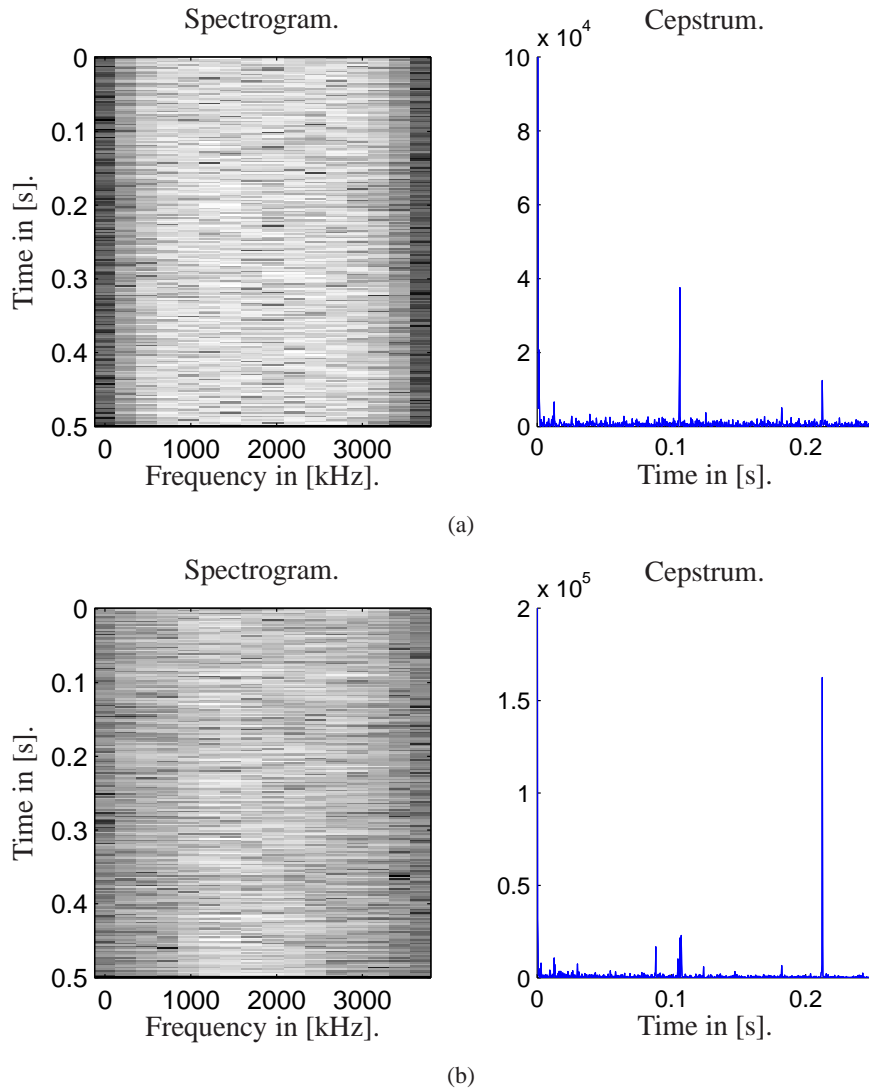


Figure 6: Spectrograms and cepstra of both a high SNR and a low SNR STANAG-4285 transmission. The dimensions of the spectrogram are equivalent to the dimensions of X_M .

Results of the transmission scanner.

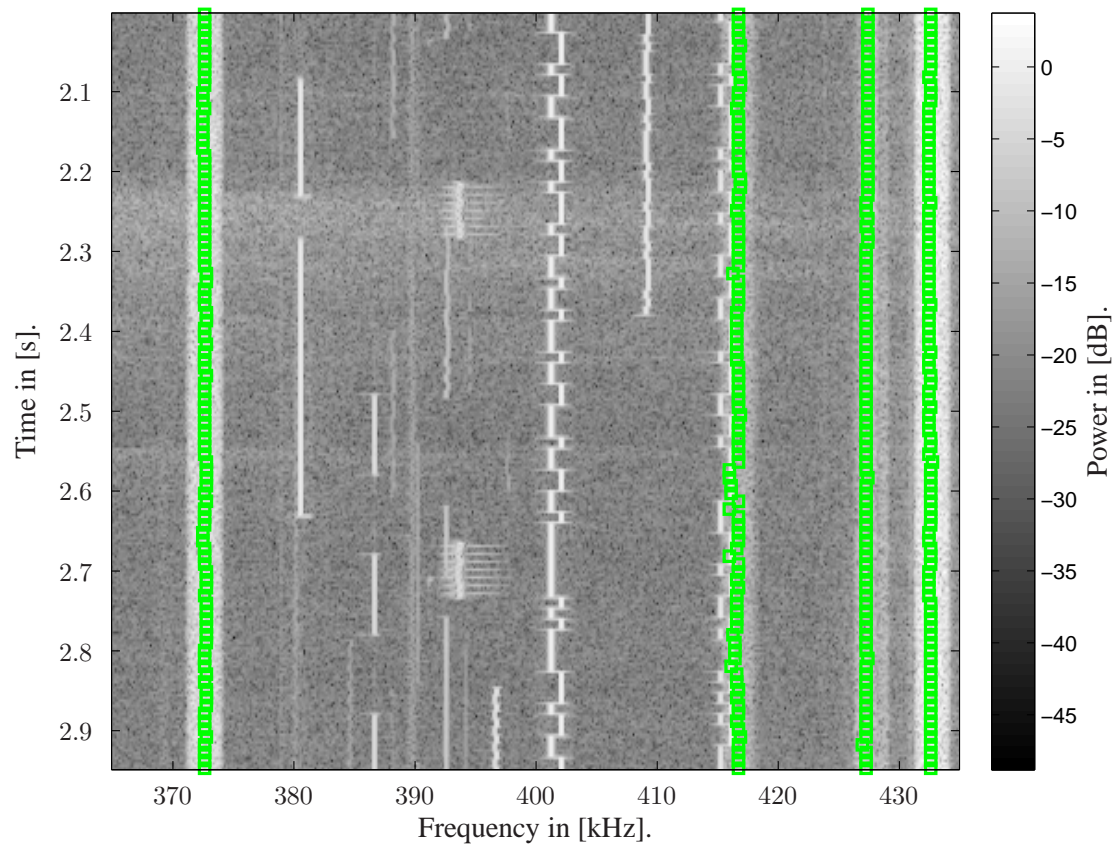


Figure 7: Part of an absolute, logarithmic wideband spectrogram. It contains the results of the transmission scanner, marked as green boxes. This classifier has been trained with a combination of f_{Haar} and f_{Ceps} . Every STANAG-4285 transmission has been found. There is no incorrect hit in this part of the wideband spectrogram.

